Spallation reaction study for fission products in nuclear waste: Cross section measurements for ^{137}Cs, ^{90}Sr and ^{107}Pd on proton and deuteron

He Wang[1,a], Hideaki Otsu[1], Hiroyoshi Sakurai[1], DeukSoon Ahn[1], Masayuki Aikawa[2], Takashi Ando[3], Shouhei Araki[4,1], Sidong Chen[1], Nobuyuki Chiga[1], Pieter Doornenbal[1], Naoki Fukuda[1], Tadaaki Isobe[1], Shunsuke Kawakami[5,1], Shoichiro Kawase[4,6], Tadahiro Kin[4], Yosuke Kondo[7], Shupei Koyama[3], Shigeru Kubono[1], Yukie Maeda[5], Ayano Makinaga[8,9], Masafumi Matsushita[6], Teiichiro Matsuzaki[1], Shinichiro Michimasa[6], Satoru Momiyama[3], Shunsuke Nagamine[3], Takashi Nakamura[7], Keita Nakano[4,1], Megumi Niikura[3], Tomoyuki Ozaki[7], Atsumi Saito[7], Takeshi Saito[3], Yoshiaki Shiga[10,1], Mizuki Shikata[7], Yohei Shimizu[1], Susumu Shimoura[6], Toshiyuki Sumikama[1], Pär-Anders Söderström[1], Hiroshi Suzuki[1], Hiroyuki Takeda[1], Satoshi Takeuchi[1], Ryo Taniuchi[3], Yasuhiro Togano[7], Junichi Tsubota[7], Meiko Uesaka[1], Yasushi Watanabe[1], Yukinobu Watanabe[4], Kathrin Wimmer[3,6,1], Tatsuya Yamamoto[5,1], and Koichi Yoshida[1]

[1] RIKEN Nishina Center, 2-1 Hirosawa, Wako, Saitama 351-0198, Japan
[2] Faculty of Science, Hokkaido University, Sapporo 060-0810, Japan
[3] Department of Physics, University of Tokyo, 7-3-1 Hongo, Bunkyo, Tokyo 113-0033, Japan
[4] Department of Advanced Energy Engineering Science, Kyushu University, Kasuga, Fukuoka 816-8580, Japan
[5] Department of Applied Physics, University of Miyazaki, Miyazaki 889-2192, Japan
[6] Center for Nuclear Study, University of Tokyo, RIKEN campus, Wako, Saitama 351-0198, Japan
[7] Department of Physics, Tokyo Institute of Technology, 2-12-1 Ookayama, Meguro, Tokyo 152-8551, Japan
[8] JEin institute for fundamental science, NPO Einstein, Kyoto 606-8317, Japan
[9] Graduate School of Medicine, Hokkaido University, Sapporo 060-8648, Japan
[10] Department of Physics, Rikkyo University, 3-34-1 Nishi-Ikebukuro, Toshima, Tokyo 172-8501, Japan

Abstract. Spallation reactions for the long-lived fission products ^{137}Cs, ^{90}Sr and ^{107}Pd have been studied for the purpose of nuclear waste transmutation. The cross sections on the proton- and deuteron-induced spallation were obtained in inverse kinematics at the RIKEN Radioactive Isotope Beam Factory. Both the target and energy dependences of cross sections have been investigated systematically. and the cross-section differences between the proton and deuteron are found to be larger for lighter fragments. The experimental data are compared with the SPACS semi-empirical parameterization and the PHITS calculations including both the intra-nuclear cascade and evaporation processes.

1. Introduction

The role of nuclear power has been emphasized since the middle of the twentieth century. The nuclear safety and security are, however, matters of concern to the entire world. One of the major issues is the management on the radioactive waste in the spent nuclear fuel produced from the nuclear power plant.

In recent years, a research and development has been performed using the partitioning and transmutation technology for the reduction of the high-level radioactive waste (HLW) [1] and for the resource recycling from the spent nuclear fuel [2]. Long-lived fission products (LLFPs) and minor actinides (MA) are two main components in HLW. The transmutation for MA has been widely discussed in a concept of using the accelerator-driven system. The study for the LLFP transmutation is limited.

The transmutation on the LLFP nuclei ^{137}Cs, ^{90}Sr and ^{107}Pd have received much attention. ^{137}Cs and ^{90}Sr have large weight fractions (40%) in LLFP and they are known to as the heat generator in high-level radioactive waste [1]. Due to their relatively short half lives of 30 years [3], ^{137}Cs and ^{90}Sr have large radiotoxicities. Indeed, the radiotoxicities in these two LLFP nuclei are predominant (more than 90%) in the first 100 years after the reprocessing of spent fuel. The palladium metal is one of useful materials in HLW but it has a radioactive isotope ^{107}Pd, which is a long-lived fission product with a half-life of 6.5×10^6 years [3]. In considering a possible mechanism for the reduction in the radioactivities of ^{137}Cs, ^{90}Sr and ^{107}Pd, the related nuclear reaction data are very scarce. Thermal neutron capture reactions were once investigated for these three LLFP nuclei [4–6].

In the present work, the spallation reactions have been performed for ^{137}Cs, ^{90}Sr and ^{107}Pd in the aspect of nuclear waste transmutation for LLFP. The inverse reaction technique was adopted in the present work: the LLFP beams were used and proton/deuteron-induced reactions were conducted by using proton and deuteron targets. The technique allows us to avoid the difficulties associated with

[a] e-mail: wanghe@ribf.riken.jp

Table 1. List of targets used in the present work.

Target	Thickness (mg/cm^2)	Experimental settings in BigRIPS
CH_2	179.2	^{137}Cs and ^{90}Sr at 185 MeV/nucleon, ^{107}Pd at 196 and 118 MeV/nucleon
CD_2	218.2	^{137}Cs and ^{90}Sr at 185 MeV/nucleon, ^{107}Pd at 196 and 118 MeV/nucleon
C	226.0	^{137}Cs and ^{90}Sr at 185 MeV/nucleon, ^{107}Pd at 118 MeV/nucleon
C	317.2	^{107}Pd at 196 MeV/nucleon

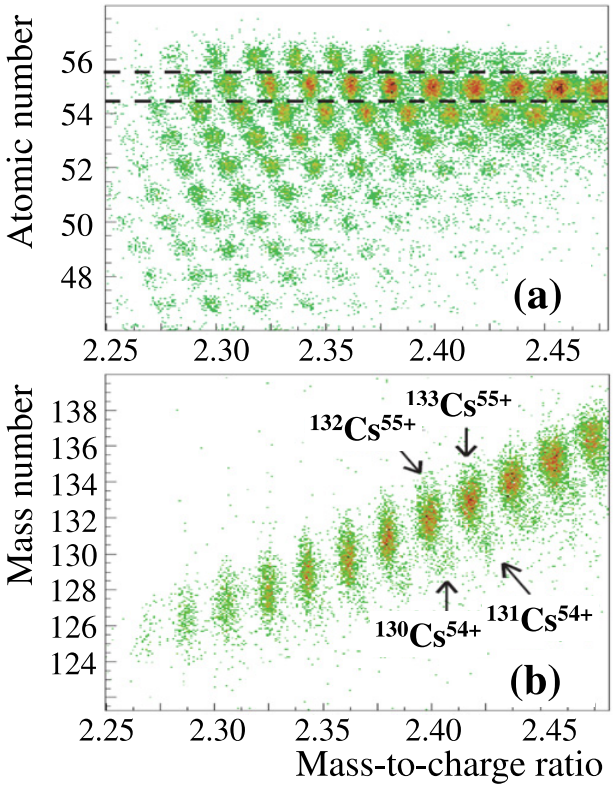

Figure 1. Particle identification plots for the ZeroDegree spectrometer. Panel (a) displays a two-dimensional plot of Z versus A/Q for the reaction residues produced from ^{137}Cs. The horizontal dashed lines indicate the Z gate which was used for selecting the Cs isotopes. In Panel (b), the two-dimensional plot of A versus A/Q is shown for the Cs isotopes. The fully stripped ions could be separated from the $Q = Z - 1$ events.

using a highly radioactive target, to identify the reaction products unambiguously, and to study systematically the target dependence of reactions. The present reaction study enables us to provide high-quality data for a possible solution to the LLFP transmutation.

2. Experiment

The experiment was performed at the RIKEN Radioactive Isotope Beam Factory, operated by RIKEN Nishina Center and the Center for Nuclear Study, University of Tokyo. The secondary beams were produced by in-flight fission of a ^{238}U beam at 345 MeV/nucleon incident on a 1-mm-thick beryllium target located at the object point of the BigRIPS separator [7]. Several BigRIPS settings were applied to optimize the transmission of ^{137}Cs, ^{90}Sr and ^{107}Pd, respectively. The particle identification for the secondary beams was made event-by-event by measuring the time of flight (TOF), the magnetic rigidity ($B\rho$), and the energy loss (ΔE) as described in Refs. [8,9] with similar experimental setups. The beam energies were both 185 MeV/nucleon for ^{137}Cs and ^{90}Sr in front of the secondary targets. For ^{107}Pd, the data were taken at both 196 and 118 MeV/nucleon.

To induce the secondary reactions, three types of targets were used. They were CH_2, CD_2 [10] and natural carbon. The target thicknesses are summarized in Table 1. In addition, data were taken by using the target holder with no target-material inserted (empty-target), in order to measure the background contribution.

The reaction residues were collected and analyzed by the ZeroDegree spectrometer [7]. In order to cover a broad range of fragments, several different magnetic rigidity ($B\rho$) settings were applied: -9%, -6%, -3%, 0%, and $+3\%$ relative to the $B\rho$ value of the beam. Thus, a sufficient overlap was obtained for neighboring settings. The particle identification was made again using the TOF-$B\rho$-ΔE method in a similar way to BigRIPS. In addition, the mass number A was deduced from the TOF information and a total kinetic energy (TKE) measurement using a $LaBr_3$(Ce) scintillator placed at the final focus of the ZeroDegree spectrometer for the identification of different charge states.

An example of the particle identification for reaction products detected by the ZeroDegree spectrometer is shown in Fig. 1 for the ^{137}Cs secondary beam on the carbon target. It is noted that the fully-stripped ions are contaminated by the lighter fragments with hydrogen-like ($Q = Z - 1$) charge states. In Fig. 1(b), a two-dimensional plot of A versus A/Q is shown and the plot was obtained by selecting the events within $Z = 55 \pm 0.5$, as indicated by the horizontal dashed lines in Fig. 1(a). Using this technique, the fully-stripped ions were unambiguously distinguished from the other charge states.

3. Results

The isotopic distributions of cross sections for the different elements produced by the ^{137}Cs and ^{90}Sr beams on proton and deuteron are displayed in Figs. 2 and 3, respectively. The proton- and deuteron-induced cross sections (σ_p and σ_d) were deduced from the measurements using the CH_2 and CD_2 targets, respectively, after subtracting the contributions from carbon (using data from the C target run) and beam-line materials (using data from the empty-target run). The data analysis for ^{107}Pd is ongoing.

Figures 2(a) and 3(a) correspond to the charge-pickup reactions. In this channel, the σ_p values are larger than the σ_d ones. It was also found that σ_p is larger than σ_d for the charge-pickup reaction channel of ^{136}Xe [12] at a high reaction energy. Isotopes close to the projectile in mass, such as Cs and Xe (Sr and Rb) in the ^{137}Cs (^{90}Sr) case, are mainly produced from the so-called "peripheral" reactions, where neutron evaporation dominates [14]. For these isotopes, as displayed in Panels (b) and (c) in Figs. 2 and 3, both σ_p and σ_d keep an almost constant value

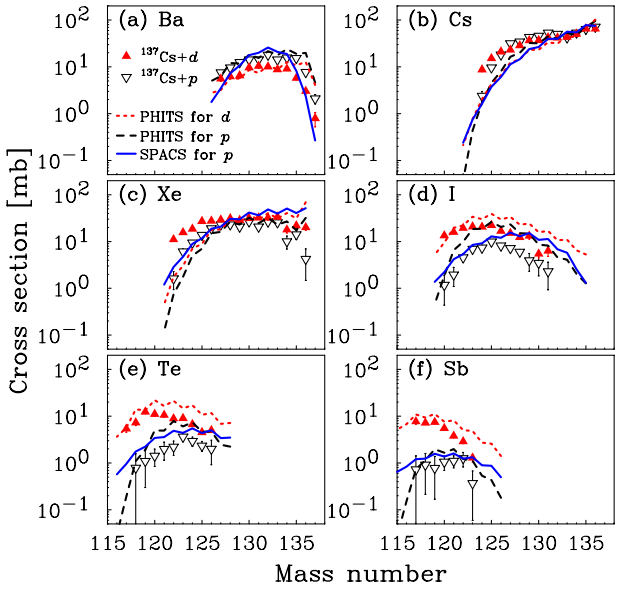

Figure 2. The isotopic cross section of residual nuclei from Sb to Ba produced by the reactions ^{137}Cs + p (down-triangle) and ^{137}Cs + d (up-triangle) at 185 MeV/nucleon. The dashed and dotted lines indicate the PHITS [15] calculations on proton and deuteron, respectively. The SPACS results on proton (solid) are displayed for comparison.

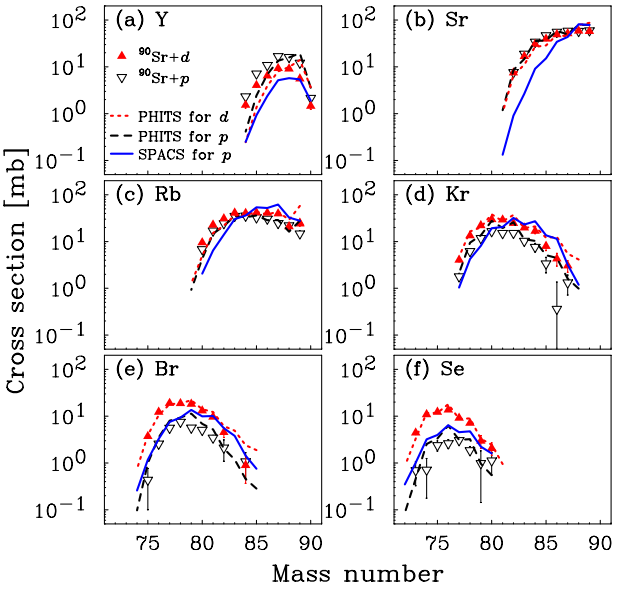

Figure 3. Same as Fig. 2, but for the nuclei from Se to Y produced by ^{90}Sr.

over a wide range of mass numbers and then slightly decrease for the neutron-deficient side. For other elements, the isotopic distributions show bell shapes as displayed in Panels (d)–(f) in Figs. 2 and 3. It was suggested that the position of the maximum is determined by the competition between the evaporation of protons and neutrons [11]. In addition, it is found that σ_d becomes larger than σ_p in these channels and their difference increases towards the neutron-deficient side for the lighter products. As the light-mass products are probably produced by a central collision, this difference between σ_d and σ_p might be related to the energy deposited. In the central collision, the cross sections depend on the energy deposited. At the same reaction energy, more energy can be deposited in the deuteron-induced reaction than that for proton because the deuteron has two nucleons. Thus, the production cross section on deuteron is larger than those on proton for the light products.

The spallation reaction is known to proceed through a two stage processes: the first stage is dominated by the nucleon-nucleon collisions, and followed by the de-excitation of pre-fragments. These two stages are commonly described by intra-nuclear cascade model and an evaporation model, respectively. For a quantitative understanding of the isotopic distribution, a theoretical calculation including these two processes was performed using the particle and heavy ion transport code system (PHITS) [15]. In the PHITS calculation, the cascade and evaporation processes were simulated by using the Intranuclear Cascade model of Liège (INCL4.6) [17] and the generalized evaporation model (GEM) [18], respectively.

The PHITS calculations reproduce the experimental systematic trends well as shown in both Figs. 2 and 3. PHITS overestimates the cross sections on the neutron-rich sides for some low-Z products, such as I, Te and Sb, as shown in Fig. 2(d)–(f). In addition, the odd-even staggering effect is overestimated by PHITS.

The experimental data were also compared to the SPACS semi-empirical parameterization [16], which has been recently developed to suit proton- and neutron-induced spallation reactions. The SPACS results are in a reasonable agreement with the isotopic distribution for the proton-induced cross sections. An underestimation is found for the Cs and Sr isotopic chains, as shown in Panel (b) in Figs. 2 and 3. In addition, SPACS overestimates the cross sections in the neutron-rich side for the I, Te and Sb isotopic chains in the ^{137}Cs case, as displayed in Panels (d)–(f) of Fig. 2, and the ones for Kr, Br and Se produced from ^{90}Sr, as shown in Panels (d)–(f) of Fig. 3.

The total spallation cross sections on proton and deuteron are important to evaluate the potential of spallation reaction for the LLFP transmutation. The cross sections for the proton and deuteron were determined to be 1110(17) mb and 1300(15) mb for ^{137}Cs, and 785(10) mb and 998(10) mb for ^{90}Sr [13] by integrating the isotopic distributions in Figs. 2 and 3, respectively. These total spallation cross sections are larger than their thermal neutron-capture cross sections of 270 mb [4] and 10 mb [5]. The large total cross sections indicates that the spallation reaction could be a promising mechanism for the transmutation of ^{137}Cs and ^{90}Sr.

The number of radioactive nuclei with long half-lives created in the spallation reaction is important to evaluate the reduction of radiotoxicities after the reaction. Among the reaction products, the long-lived isotopes ^{135}Cs and ^{79}Se are the main components of radioactivity following the spallation of ^{137}Cs and ^{90}Sr, respectively. Their production cross sections on proton are around 64 mb and 1 mb, respectively. Since the total spallation cross sections for both ^{137}Cs and ^{90}Sr are around 1 barn, the spallation reaction will lead to a considerable reduction in the number of LLFP elements. The half lives of ^{135}Cs and ^{79}Se are 2.3×10^6 and 6.5×10^4 years, respectively, which are much longer than those for ^{137}Cs and ^{90}Sr. Therefore, after the spallation reactions, the radiotoxicities in ^{137}Cs and ^{90}Sr will be reduced.

4. Summary

In summary, spallation reactions have been studied for the long-lived fission products ^{137}Cs, ^{90}Sr and ^{107}Pd on proton and deuteron in inverse kinematics at RIBF. Cross sections on proton and deuteron were obtained at 185 MeV/nucleon for ^{137}Cs and ^{90}Sr. It is found that the difference between σ_d and σ_p becomes larger towards the neutron-deficient side for the light-mass products. An overall agreement is found between the experimental data and the PHITS calculation including both the intra-nuclear cascade and evaporation processes. The SPACS parameterization also shows a reasonable agreement with the results of the proton-induced reactions. The total spallation cross sections on both proton and deuteron are found to be larger than those for the neutron-capture reactions, suggesting the spallation reaction is promising for the transmutation of ^{137}Cs and ^{90}Sr.

We thank the accelerator staff of RIKEN Nishina Center for providing the U primary beam. This work was partly supported by ImPACT Program of Council for Science, Technology and Innovation (Cabinet Office, Government of Japan).

References

[1] Implication of Partitioning and Transmutation in Radioactive Waste Management, IAEA Technical Reports Series **435** (2004)
[2] K. Nishihara et al., J. Nucl. Sci. Technol. **45**, 84 (2008)
[3] W.S. Yang et al., Nucl. Sci. Eng. **146**, 291 (2004)
[4] H. Wada et al., J. Nucl. Sci. Technol. **37**, 827 (2000)
[5] S. Nakamura et al., J. Nucl. Sci. Technol. **38**, 1029 (2001)
[6] S. Nakamura et al., J. Nucl. Sci. Technol. **44**, 103 (2007)
[7] T. Kubo et al., Prog. Theor. Exp. Phys. **2012**, 03C003 (2012)
[8] T. Ohnishi et al., J. Phys. Soc. Jpn. **79**, 073201 (2010)
[9] N. Fukuda et al., Nucl. Instrum. Methods Phys. Res. B **317**, 323 (2013)
[10] Y. Maeda, et al., Nucl. Instrum. Methods Phys. Res. A, **490**, 518 (2002)
[11] W. Wlazło et al., Phys. Rev. Lett. **84**, 5736 (2000)
[12] J. Alcántara-Núñez et al., Phys. Rev. C **92**, 024607 (2015)
[13] H. Wang et al., Phys. Lett. B **754**, 104 (2016)
[14] J. Benlliure et al., Phys. Rev. C **78**, 054605 (2008)
[15] T. Sato et al., J. Nucl. Sci. Technol. **50**, 913 (2013)
[16] C. Schmitt, K.-H. Schmidt, and A. Kelić-Heil, Phys. Rev. C **90**, 064605 (2014)
[17] A. Boudard, J. Cugnon, S. Leray, and C. Volant, Phys. Rev. C **87**, 014606 (2013)
[18] S. Furihata, Nucl. Instru. Methods B **171**, 251 (2000)